In Situ Measurements of Chemical Sensor Film Dynamics by Spectroscopic Ellipsometry. Partitioning of a Chromophore

Imants Zudans, William R. Heineman, and Carl J. Seliskar*

Department of Chemistry, P.O. Box 210172, University of Cincinnati, Cincinnati, Ohio 45221-0172
Received: August 18, 2003; In Final Form: May 27, 2004

Spectroscopic ellipsometry data are presented that describe the dynamics of the partitioning of a model chromophore ($Ru(bpy)_3^{2+}$) into a thin porous solid film (Nafion). Backside optical interrogation permitted the study of the film at wavelengths where the bathing solution containing the chromophore significantly absorbed light. Data acquired in situ while the model chromophore $Ru(bpy)_3^{2+}$ partitioned into the film were successfully interpreted using an optical multilayer layer model. This model was constructed by sequential experimental examination of the individual component layers of the system. A quantitative description of the dynamic film was achieved by assembling a model film layer that contained Tauc-Lorentz oscillators to describe both the real and imaginary parts of the refractive index using the Kramer-Kronig relationship. Subsequent analysis of experimental data using the model resulted in a quantitative description of how the optical constants and thickness of the film changed as chromophore $Ru(bpy)_3^{2+}$ partitioned into it from solution. The film's thickness also changed during the course of the partitioning. On the first incorporation of the chromophore, the film contracted and then, as the film approached equilibrium with the bathing solution, re-expanded. Digital simulations of three different chromophore partitioning modes were presented. Analysis of Δ vs Ψ plots for the three simulated modes strongly supports a simple uniform optical layer model description of the partitioning process for the $Ru(bpy)_3^{2+}$−Nafion film system under the prevailing experimental conditions. Overall, the results gave new insights into the acquisition of the data for and associated interpretation of the chromophore-film partitioning process.

1. Introduction

The incorporation of a solution phase molecule (analyte) into a thin porous solid film on a transducer is a process that is fundamental in chemical sensing. Much attention has been and will continue to be paid to the formulation and preparation of such films. The literature is rich with studies of these films that have been examined by a wide variety of techniques including QCM,[1−5] absorbance and fluorescence spectroscopies,[6−10] and single wavelength ellipsometry.[11] In recent years the vintage technique of single wavelength ellipsometry has been extended to spectroscopic ellipsometry; that is, ellipsometry done over a broad range of wavelengths. Because of our interest in the spectroelectrochemical sensor[12,13] we have turned to spectroscopic ellipsometry as a noninvasive technique that might be useful in studying the dynamics of thin porous solid films exposed to solution, in particular, those films fabricated from optical quality composites[14,15] that are candidates for use in optical chemical sensors.

In a first paper[16] we reported the quantitative description of the dynamics of acid etching of a thin indium tin oxide film measured by spectroscopic ellipsometry. In that work we established a procedure for systematically measuring the initial and final states of the system by ex situ measurements. Armed with that information and backside optical interrogation, we then demonstrated how one could quantitatively describe the dynamics of that optical multilayer system. In subsequent work we grappled with the problem of how to construct a liquid flow cell free from significant strain effects that would allow separation of the reflections from important interfaces from "trivial" reflections, that is, ones not containing information about film processes. In this paper we describe this technique and give an example of its use. We have chosen to study a system consisting of a Nafion thin film and aqueous $Ru(bpy)_3^{2+}$ (a model analyte). Together these two components form a model chemical system that exhibits a degree of selective chemical partitioning (cation exchange) of a chromophore ($Ru(bpy)_3^{2+}$) into a porous solid film (Nafion), all of which have quantifiable optical constants. Our purpose was not to study Nafion and $Ru(bpy)_3^{2+}$ per se, but rather to use them as tools to develop a noninvasive quantitative optical technique that could be applied to thin porous solid sensor films of considerably more interest to us.

2. Experimental Details

2.1 Chemicals and Materials. Tris(2,2′-bipyridine) ruthenium(II) chloride hexahydrate ($Ru(bpy)_3Cl_2$, Aldrich), Nafion (5% solution in lower aliphatic alcohols and 10% water, Aldrich), CH_2Cl_2 (Fisher Scientific), and methanol (Fisher Scientific) were used as purchased. Deionized water was prepared with a Barnstead water purification system and used to prepare all solutions. Gaskets were cut from silicone sheeting (0.010 in thick, gloss/gloss surface, Specialty Manufacturing, Inc., Saginaw, MI). Nalgene 50 silicone tubing (0.125 in ID × 0.250 in OD, Fisher Scientific) was used to deliver solutions into the ellipsometry cell. Fine annealed SF11 glass slabs were purchased from Schott, cut into pieces, and polished as needed.

2.2 Instrumentation. A Buehler Ecomet variable speed grinder-polisher with an Automet 2 power head was used to grind and polish glass substrates. An HP 8453 diode array spectrophotometer was used to acquire UV−Vis spectra. A Cole-Parmer Instruments Co. peristaltic pump (model 7021-24) was used to circulate liquids within the flow cell. A J. A. Woollam, Inc. variable angle spectroscopic ellipsometer (vertical configuration) was used for all ellipsometric measurements. This instrument was equipped with an adjustable retarder (Auto

10.1021/jp0364553 CCC: $27.50
Published on Web 07/03/2004

Retarder) that enabled measurements of Ψ and Δ to be made over the full range (0−90 and 0−360 degrees, respectively), and also permitted depolarization of the light to be measured. However, for time-based studies the adjustable retarder was used in the fast mode in which depolarization is not measured. J. A. Woollam, Inc. WVASE32 software was used for modeling ellipsometric data using published techniques.[17,18] Goodness-of-fit was expressed as mean squared error (*MSE*) between experimental and predicted data (normalized by the standard deviations of experimental data). Thus, a smaller *MSE* value represents better agreement between experimental and predicted data.

In a previous paper we described a liquid flow cell for spectroscopic ellipsometry and demonstrated its use for measuring film thickness, in situ, during the acid etching of an ITO film on glass.[16] A very similar cell was used for this work except that the liquid volume of the cell used was made smaller than that used previously so as to accept thick glass substrates. Details of the cell construction can be found elswhere.[16,19]

2.3 Preparation of Films on Substrates. Fine annealed Schott SF11 glass was rough cut in 12 × 150 × 8 mm pieces and then into 12 × 50 × 8 mm pieces and these substrates were polished in house (the procedure may be found in Supporting Information). The typical substrate thickness was between 6 and 7 mm after polishing. The finished substrates were cleaned by wiping with lens paper soaked with dichloromethane and then lens paper soaked with methanol, rinsing with deionized water, and then cleaning with Isoclean cleaning solution (surfactant, Isolab, Inc). Finally, the substrates were rinsed with a large volume of deionized water and dried with lens paper. Films on clean substrates were prepared by spin-coating 5% Nafion solution onto them using a Headway spincoater operated at 1000 rpm for 30 s. Prior to use, films were stored under ambient conditions for at least 12 h.

3. Results and Discussion

We are not aware of any reports of spectroscopic ellipsometry studies of the dynamics of the partitioning of a chromophore into a thin solid film. As a result, we asked ourselves two questions as we began these studies. First, can we rigorously model the dynamics of the partitioning of a chromophore into a thin film that also changes in physical extent? Second, assuming that we can quantitatively model the chromophore partitioning into such a film, what can we learn about the partitioning process from the ellipsometry parameters? Our general approach in answering these questions was to first devise an ellipsometry technique that allowed us to maximize the information obtained about the partitioning process and then to systematically develop an optical modeling strategy that led to well-defined optical and physical constants for the film-chromophore system in time.

3.1 Backside Optical Interrogation. Figure 1 illustrates the optical configuration for "backside" measurements. Incident light (IL) strikes the substrate's first surface where part of the light is reflected back (front reflection, FR). This is the reflection that is typically measured in ellipsometry experiments. The other portion of the incident beam is transmitted into the substrate and eventually encounters the film/solution interface. From there it is partly transmitted into the solution (transmitted beam, TB1) and partly reflected back into the film/glass substrate. As can be seen from the figure, the back-reflected beam reaches the glass/air interface where part of it escapes (back reflection, BR1) and the remainder is reflected back into the glass. Light continues to reflect at interfaces subsequently producing beams TB2, BR2, etc., until all the intensity is quenched. At each of the reflection points, the optical path is split and, therefore, each

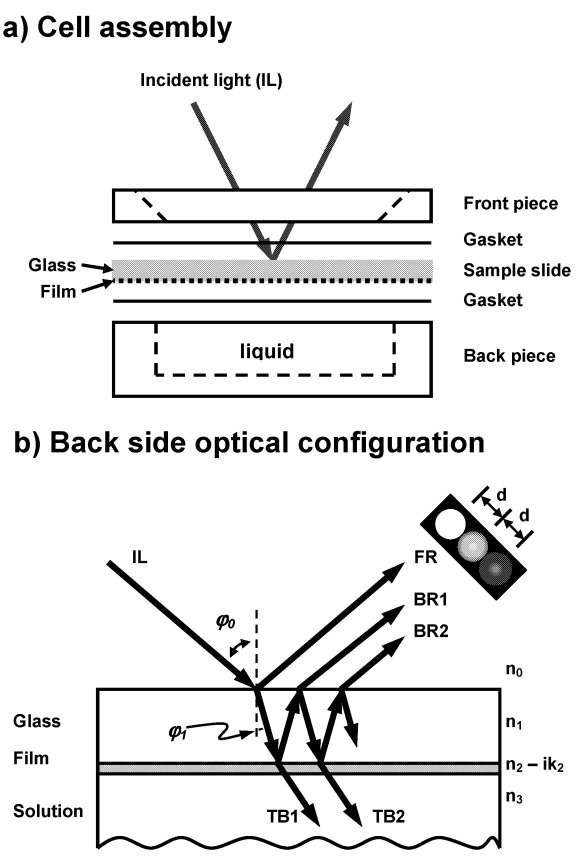

Figure 1. Liquid flow cell experimental details are shown: (a) flow cell components and assembly; (b) illustration of the backside optical configuration.

next beam exiting glass in the direction of a detector (on the air side of the substrate) is weaker than the previous (BR2 weaker than BR1, etc.). The front reflection (FR) is the strongest, but since it does not encounter the glass-film interface, it contains no information about the film. Applied successively to all surfaces, the Fresnel equations and Snell's law[20] can be used to calculate the intensities of reflections in a backside ellipsometry measurement configuration (FR, BR1, BR2).

The first reflection from the back surface (BR1) is the most intense and the first to contain information about the film. The diameter of the probe beam in the ellipsometer used is about 3 mm. If the glass substrate is thin (1 mm or less) then beams FR, BR1, and BR2 overlap on the detector. In such a case, the relatively small signal from the back-surface (film) reflection is overwhelmed by the much larger signal arising from the front surface. Due to this overlap, the sensitivity of measurements to film properties is significantly decreased. Nonetheless, as we have demonstrated with ITO acid etching studies,[16] in certain cases a film can be successfully monitored using such a configuration.

Equation 1 describes the displacement, *d*, of the centers of the beams reflected at the interfaces of the glass substrate (FR1, BR1, and BR2) in the direction of the detector as a function of the angle of incidence, φ_0, the glass substrate refractive index, n_1, and its thickness, *t*.

$$d = t \times \frac{\sin(2\varphi_0)}{n_1} \times \left(1 - \frac{\sin^2(\varphi_0)}{{n_1}^2}\right)^{-1/2} \qquad (1)$$

The function *d* goes through a maximum as the angle φ_0 increases from 0 to 90 degrees. The position of the maximum

depends on the refractive index of the glass, n_1. If a sufficiently thick substrate is used (6−7 mm), reflections FR, BR1, and BR2 do not overlap at certain angles of incidence. For example, for a 6-mm thick substrate with refractive index 1.7 at a 60° angle of incidence, the separation of the reflected beams is 3.6 mm center-to-center. Thus, one of these beams can be selected (by using an iris) for monitoring. It is obvious that beam BR1 should be chosen if the film is to be studied since measurements would be more sensitive to the back-surface of the glass (where the film is) as compared to the case where all beams overlap. We have used beam BR1 for in situ experiments described in this paper.

3.2 Spectroscopic Ellipsometry and Optical Modeling of the System. Ellipsometry results are usually presented as two parameters, Ψ and Δ, which relate how light's electric field component parallel to the plane of incidence (p polarized) is reflected relative to that perpendicular to the plane of incidence (s polarized). These parameters[20,21] are calculated from the complex reflectance ratio ρ given in Equations 2 and 3, where R and T are the complex amplitudes of reflected or transmitted light, respectively.

$$\tan\Psi = |\rho| = \frac{|R_p|}{|R_s|} = \frac{|T_p|}{|T_s|} \tag{2}$$

$$\Delta = \tan^{-1}\frac{\mathrm{Im}(\rho)}{\mathrm{Re}(\rho)} \tag{3}$$

Experimentally determined Ψ and Δ values are deconvoluted using a specific optical model to extract the sample's properties. In the modeling process, a specific physical structure composed of layers and interfaces is assumed and used to calculate the complex reflectance ratio ρ, which is then compared iteratively to experimental data. Optimization routines are used that adjust the computational model properties (e.g., film thickness) to minimize differences between experimental and calculated results. Spectroscopic ellipsometry determines the reflectance ratio ρ as a function of wavelength over a broad region of the spectrum, enabling studies of more complex samples and also making data interpretation less ambiguous.

In this paper we refer to a mathematical description (collection of optical and physical constants) of a single layer (film, substrate, solution, etc.) as an *optical layer*. A collection of such optical layers bounded by interfaces that describes the structure of a given system for ellipsometric data analysis purposes will be referred to as an *optical model*. Each layer's optical constants are described at each wavelength by a complex refractive index, $\bar{n} = n - ik$ in which the real part, n, is an inverse measure of the phase velocity of light in the layer compared to vacuum and is often referred to simply as the refractive index. The complex part of the refractive index, k, is a measure of how much light is absorbed in the material and is related to the absorption coefficient α, at wavelength λ (nm) by $k = (\lambda/4\pi)\alpha$. The components n and k are not independent of each other; to model the refractive index of materials we use an optical layer model where n and k are linked by the Kramer-Kronig relation.[21] In an optical layer model that uses this relation, the extinction coefficient k is expressed as a collection of oscillators (Gaussian, Lorentz, etc.) at specified energies (or wavelengths). The refractive index profile with wavelength is then calculated from the extinction coefficient's profile with wavelength. Additionally, it is necessary to take into account absorbance from outside the region of interest since the associated oscillators can influence the refractive index in the wavelength region of interest. For example, the typical normal dispersion of the refractive index n with increasing wavelength in the visible part of the spectrum of a colorless material is due to material absorbance at short wavelengths. Normal dispersion of n is often described by the Cauchy equation:

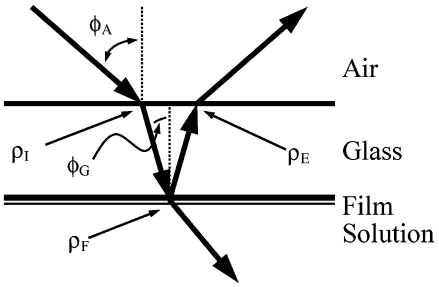

Figure 2. Illustration of backside optical system components. Angle of light in each optical medium is marked with ϕ. Complex transmittance ratio at the front surface of the glass slide is marked with ρ_I and ρ_E. Complex reflectance ratio of the glass\film\solution subsystem is marked as ρ_F.

$$n(\lambda) = A + {}^{B}/_{\lambda^2} + {}^{C}/_{\lambda^4} \tag{4}$$

Even though the absorbance spectrum outside the range of interest may not be known, for modeling purposes adding a sharply peaked oscillator with high amplitude (a pole) just outside the region of interest can model its effects in the integration. To arrive at a numerically satisfactory value of the refractive index of a material, besides the oscillators that model absorbance and a pole, a positive refractive index offset typically needs to be added to the optical layer model. This offset represents the cumulative effect of absorbance to even shorter wavelengths of the wavelength region of interest.

The changes of polarization and intensity of light interacting with a plane interface are conveniently described using a matrix formalism[20,22] as detailed in the Supporting Information.

It is convenient to describe backside ellipsometry measurements using the notation illustrated in Figure 2. The overall interaction can be separated into three contributions: (1) the transmission of the incident probe beam (also IL, Figure 1) into the glass substrate described by ρ_I; (2) the exiting beam (also BR1, Figure 1) back into ambient air described by ρ_E; and (3) the transformation of the light at the combined glass/film/solution layer-interface-layer described by ρ_F. This separation into individual contributions also allows for estimating the importance of each of these contributions. The complex reflectance ratio ρ_F and the complex transmission ratios ρ_I and ρ_E for the combined glass−film−solution interface are then calculated from the associated scattering matrix elements for s and p polarized light. In turn, the complex reflectance ratio at each wavelength for the complete optical system of layers and interfaces using backside ellipsometry is given by the product

$$\rho = \rho_I \rho_F \rho_E \tag{5}$$

With this value of ρ, ellipsometry parameters Ψ and Δ can then be calculated for each wavelength using Equations 2 and 3.

3.3 Layer Characterization and the Determination of a Global Optical Layer Model. At the outset it is important to state that all optical layers used for modeling experimental results consisted of optically uniform (isotropic) layers. Our initial strategy was to assemble a multilayer optical model from individual determinations ex situ of the various single optical layers that make up the optical system (SF11 base glass, Nafion film with and without water of hydration, solution with and without chromophore, etc.). The multilayer model was then

augmented with a Nafion film model that accounted for Ru(bpy)$_3^{2+}$ incorporation and the resultant model for the complete system, designated the *global optical model*, could be applied to the Nafion film with or without Ru(bpy)$_3^{2+}$ incorporation and either under static or dynamic experimental conditions.

The SF11 base glass optical constants were determined ex situ by examination of an uncoated SF11 glass slide using only front reflection FR1 (Figure 1). A spectroscopic scan from 300 to 1100 nm with a step size of 10 nm was performed at angles 58° to 64° with a 1° increment. In this scan, light depolarization was also measured. The *optical model* for these measurements included the following *optical layers*: a surface roughness layer (5.9 nm) and a SF11 glass layer (6 mm). Ellipsometric data were fitted well and gave a *MSE* of 1.0. The need for the inclusion of a small surface roughness layer on the surface of SF11 for in-house prepared glass substrates is, most likely, due to the polishing procedure. These SF11 optical constants were used in all subsequent analyses without modification (These constants are in good agreement with the manufacturer's specifications of this glass.).

The refractive index of water was taken from the literature[23] and its extinction coefficient was set at 10^{-8}, an insignificant nonzero value necessary for software functioning. It was assumed that a small concentration of Ru(bpy)$_3^{2+}$ (10^{-5} M) and supporting electrolyte (10^{-1} M) present in the bathing solution did not change the refractive index of water itself significantly and this is in agreement with our previous studies.[3]

Dry Nafion film's refractive index was determined by modeling in situ data for Nafion on SF11 glass that were collected before water was injected into the flow cell. These data were collected at a 60° angle of incidence from 400 to 1100 nm with a 20-nm increment. A Cauchy dispersion equation (Equation 4) was used to describe refractive index dispersion (parameters A = 1.353, B = 0.0018, and C = 0). The optical model for the complete description of dry Nafion film/SF11 glass included the following layers: a surface roughness layer (6.9 nm); a SF11 glass layer (6 mm); and a film layer (334 nm). A roughness layer for the glass/film interface was not included since it did not improve the fit quality.[21] Data analysis steps are summarized in Table S1.

After the dry Nafion film was characterized, water was injected into the flow cell. To determine how the film changed as a result of this, data were acquired under the same scan conditions as for the dry film. In the *optical model*, a water layer was added as an infinite layer; that is, the resulting model was a surface roughness (6.9 nm), a SF11 layer (6 mm), a film layer (437 nm), and a water layer (infinite). Experimental data were fitted with a *MSE* of 0.9 with the coefficients in the Cauchy equation: A=1.328, B=0.0030, and C=0. Analysis of the results indicates that the Nafion film's refractive index decreased and its thickness increased by 31%. Film swelling of 30 to 37% has been routinely observed for Nafion films in our studies and these results are consistent with literature data.[24−28] These results for the Nafion film in contact with water were augmented for chromophore incorporation as will be described later.

For global modeling, it was necessary to model the Ru(bpy)$_3^{2+}$ absorbance spectrum with oscillators. The spectrum of Ru(bpy)$_3^{2+}$ in aqueous solution is shown in Figure 3 and this was fitted with an oscillator model from 290 to 1100 nm with an average deviation of 0.003 absorbance units. Seven Tauc-Lorentz oscillators[29] at different wavelengths were used to describe the spectrum. Their wavelength positions and relative amplitudes are summarized in Table S2. To describe the refractive index of the film quantitatively, a pole and an *n* offset

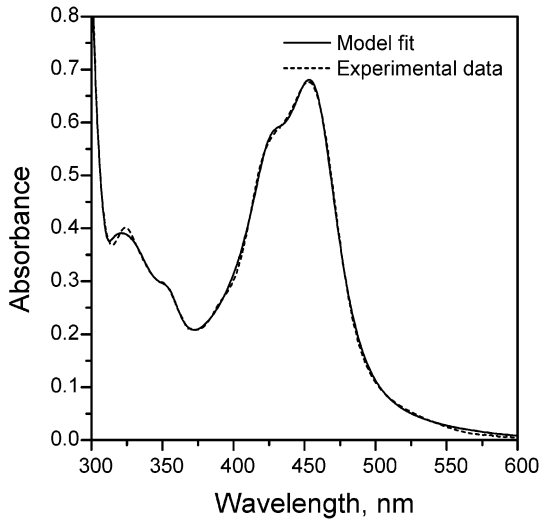

Figure 3. Experimental (dashed line) and oscillator-model fitted (solid line) absorbance spectrum of Ru(bpy)$_3^{2+}$ in water.

were added (vide supra) when ellipsometric data were fitted. As can be seen from Figure 3, the agreement between the calculated and experimental spectra is very good with the largest difference observed near 325 nm. However, the shortest experimental wavelength used for dynamic ellipsometry studies was 400 nm and for longer wavelengths than this value the agreement is exceptionally good. It is to be noted that when ellipsometric data were fitted, all seven oscillators were locked together and only their absolute collective magnitude was allowed to vary.

In situ ellipsometric data were collected at 58, 60 and 62 degrees of incidence over the region 3 eV (413 nm) to 1.25 eV (1000 nm) with a 0.025 eV increment 30 min after a Nafion film was equilibrated with Ru(bpy)$_3^{2+}$. Such instrumental scan conditions were chosen to acquire more data at the short wavelength part of the spectrum. Therefore, more data can be acquired near the Ru(bpy)$_3^{2+}$ absorption maximum (453 nm, see Figure 3) than at longer wavelengths where the chromophore does not absorb. Multiple angles of incidence provide more data for analysis, an important advantage of the backside measurement configuration over conventional liquid cells. The optical model for Ru(bpy)$_3^{2+}$-equilibrated Nafion consisted of the oscillator layer in which the combined amplitude of the oscillators, the pole magnitude, and the refractive index offset were allowed to vary in the fitting process. Data were fitted with an *MSE* of 1.3 (Table S2, Step #4). This fitted model for the hydrated film in conjunction with those of the base glass and the solution then established the basis for all subsequent analyses (i.e., the *global* optical model). As a check, the Nafion film exposed only to water was then reanalyzed by setting the collective oscillator magnitude to zero (Ru(bpy)$_3^{2+}$ not present in the film) and fitting the *n* offset. This adjusted oscillator layer also then described the data for Nafion film in water equally as well (*MSE* = 0.9, Table S2, Step #5) as the Cauchy dispersion model described earlier (*MSE* = 0.9, Table S2, Step #3). For fitting dynamic data, this global optical model was used and the refractive index offset and the oscillator magnitude were allowed to vary between values for dry film and film equilibrated with Ru(bpy)$_3^{2+}$. The optical constants of all layers are summarized in Figure 4.

Film thickness along with optical constants (*n* and *k*) were allowed to vary when dynamic data were analyzed. Since only experimental ellipsometric parameters Ψ and Δ are used in fitting dynamic experiments, there are only two unknowns at

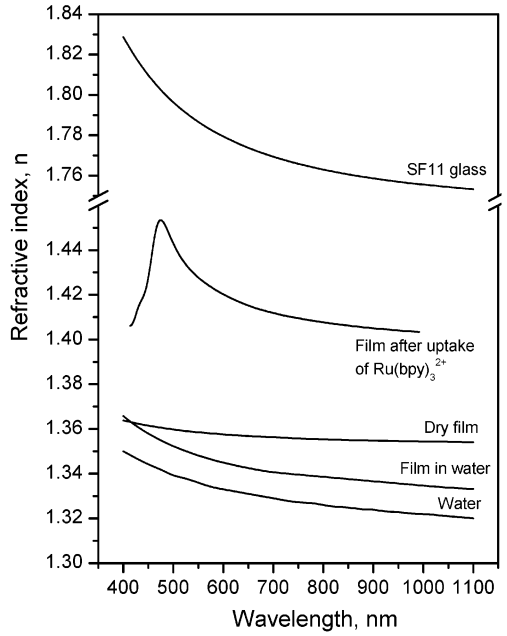

Figure 4. Refractive indices, *n*, of layer materials assuming a uniform optical layer model.

each wavelength that can be determined. However, three unknown parameters need to be determined: film thickness, refractive index (*n*), and extinction coefficient (*k*). This determination is possible because the data are obtained at many wavelengths and the oscillator-based parameterization of the optical constants was used. At long wavelengths where $Ru(bpy)_3^{2+}$ does not absorb, *k* is effectively 0. This wavelength region is useful because there are only two variables to fit, film thickness and refractive index; therefore, the data are not underdetermined. In the wavelength region where $Ru(bpy)_3^{2+}$absorbs light, the film's extinction coefficient, *k*, is nonzero and data are clearly underdetermined at every individual wavelength if the data is analyzed separately. However, both parts of the complex refractive index, *n* and *k*, are linked by the Kramer-Kronig relationship and through the oscillator model for $Ru(bpy)_3^{2+}$ absorbance. In addition, the film's thickness is essentially determined from data at wavelengths where $Ru(bpy)_3^{2+}$ does not absorb. Considering all of the above, all three film parameters (*t*, *n*, and *k*) can be determined in one experiment. This conclusion nicely illustrates the advantages of *spectroscopic* ellipsometry over single wavelength ellipsometry, where it is not possible to determine all three parameters simultaneously without additional data (such as reflection intensities).

3.4 Dynamics of $Ru(bpy)_3^{2+}$ Partitioning into Nafion Film. After a Nafion film was equilibrated with water, aqueous 10^{-5} M $Ru(bpy)_3^{2+}$ solution (with or without 0.1 M KNO_3) was injected into the flow cell and dynamic data acquisition started. To reduce $Ru(bpy)_3^{2+}$ depletion in solution near the film's surface, 200 mL of solution was continuously circulated through the cell using a peristaltic pump. Data were collected at a 60° angle of incidence from 420 to 1000 nm with a step size of 20 nm. Such scans consisted of measurements at 30 wavelengths and took 1.7 min.

Data analysis was done after the completion of the experiment and each separate wavelength scan of 30 data points was fitted individually using the global optical model. Three parameters were allowed to vary, film thickness and two parameters describing the film's optical constants (amplitude of oscillators describing $Ru(bpy)_3^{2+}$ absorption and an *n* offset). Initial values

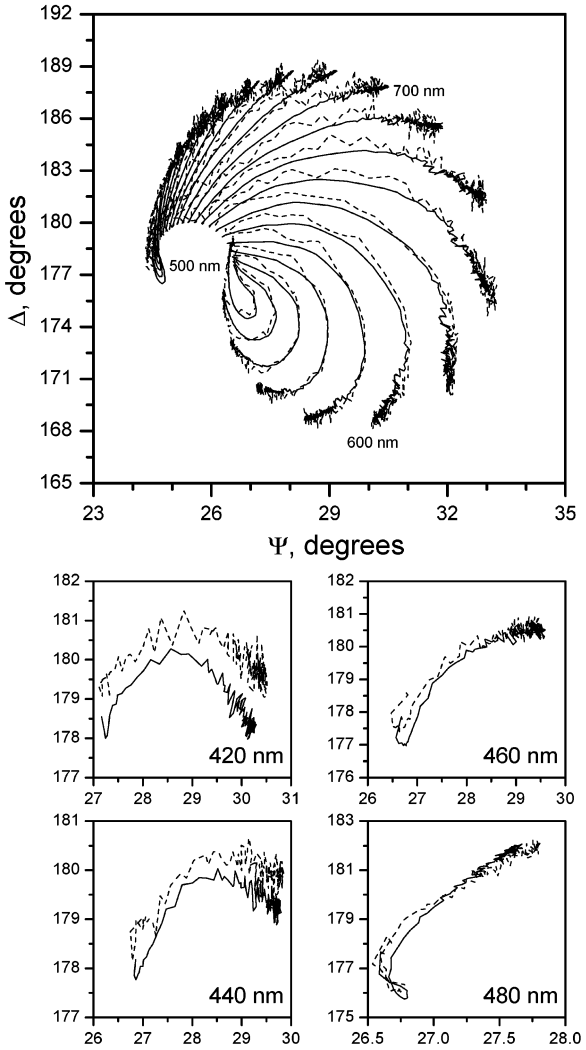

Figure 5. Δ vs Ψ plots of experimental (dashed lines) and model-predicted (solid lines) ellipsometric data: top panel, data at wavelengths from 500 to 1000 nm; bottom panels, data at wavelengths from 420 to 480 nm. Each point on these trajectories represents experimental Ψ and Δ values at a specific wavelength and time.

for all parameters were taken as those from the fitting of the Nafion film in water.

Initially, ellipsometric parameters (Δ and Ψ) change quickly as $Ru(bpy)_3^{2+}$ partitioned into the film (see Supporting Information Figure S1). As the film became saturated its properties change less and this is revealed by Δ and Ψ approaching constant values. Data at all experimental wavelengths are presented as Δ vs Ψ plots in Figure 5. Each point in these graphs represents Δ and Ψ values measured at a particular time at a particular wavelength and the curves may be thought of as trajectories in time. It is evident from Figure 5 that the overall shapes of the experimental and model trajectories generally agree. In turn, this agreement suggests that dynamic processes that occur within the film have been modeled correctly. A small constant offset of the model results from the experimental data would just indicate that some other optical layer would not be described adequately within the model. Whereas, overall disagreement would indicate that the film process was not modeled correctly. The fact that the model and experimental trajectories agree well overall strongly supports the surprising conclusion that the film is filled in such a way that the concentration of the $Ru(bpy)_3^{2+}$ increases in time *uniformly* throughout its thickness. Indeed, as will be demonstrated in a later section, simulations of alternative filling schemes where large concentration gradients are assumed

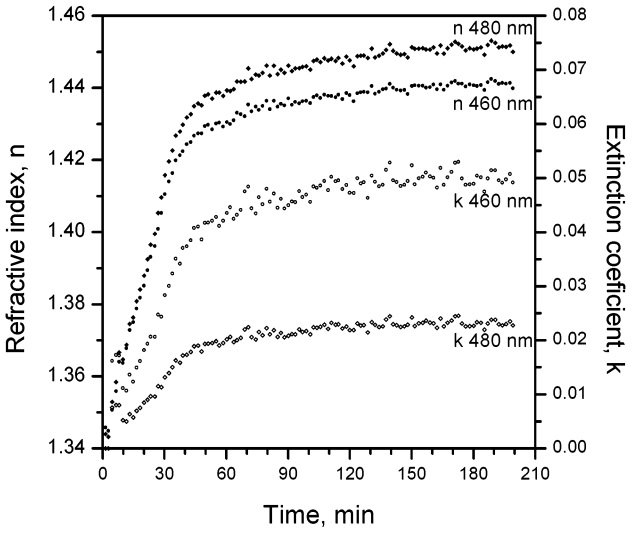

Figure 6. Refractive index and extinction coefficient vs time at two selected wavelengths for $Ru(bpy)_3^{2+}$ partitioning into Nafion film.

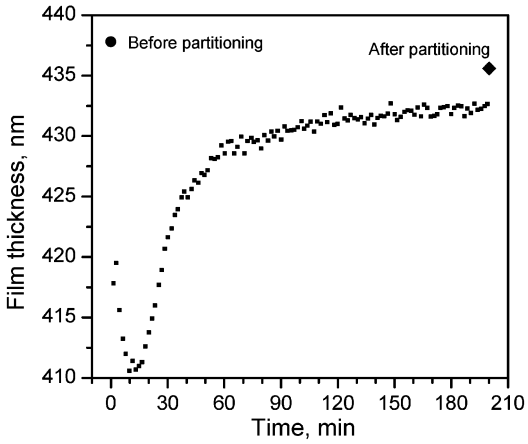

Figure 7. Nafion film thickness vs time for $Ru(bpy)_3^{2+}$ partitioning into the Nafion film from 10^{-5} M solution in aqueous 0.1 M KNO_3 solution.

for the film indicate that the associated Δ vs Ψ trajectories are distinctly different from those measured.

The coefficient *k* increases uniformly in time due to the even filling of the film with chromophore $Ru(bpy)_3^{2+}$. These extinction coefficient changes are matched by refractive index changes that show an anomalous dispersion region at the absorption maximum of $Ru(bpy)_3^{2+}$and a Cauchy-like region at longer wavelengths (see Figure 4).

Optical constant changes over time at two selected wavelengths are presented in Figure 6. Both the refractive index and extinction coefficient of the film increase very rapidly in the beginning of the experiment and start to level off about an hour after exposure of the film to $Ru(bpy)_3^{2+}$ solution. The film's refractive index change is relatively large, over 0.1 units at the absorption maximum of $Ru(bpy)_3^{2+}$ (453 nm). At other wavelengths the refractive index increased less, but the increase was significant relative to that for the film in water.

The dynamics of film thickness changes are shown in Figure 7. The results indicate that initially the film slightly contracts as $Ru(bpy)_3^{2+}$ partitions into it. The thickness of the film in water prior to the start of the uptake was determined to be 438 nm and this is indicated with a circle symbol. As the experiment progressed, the film's contraction stopped and then the film expanded to near its initial value (marked by diamond symbol, 436 nm). It must be noted that the bathing solutions for our experiment in Figure 7 contained two cations that can exchange with protons in the Nafion film, K^+ and $Ru(bpy)_3^{2+}$. Initial contraction of the film might then be explained by a faster uptake of one of these ions followed by a slower uptake of the other. The uptake or exchange of the first ion by the second could then be accompanied by film expansion. However, in equivalent experiments not discussed in detail here, where the K^+ ion was absent, very similar thickness changes were observed for $Ru(bpy)_3^{2+}$ uptake into Nafion film. One example of such an experiment is presented in the Supporting Information (Figure S2). These results seem to rule out the K^+ ion as the source of the film thickness contraction.

3.5 Testing of Alternative Chromophore-film Partitioning Models. Several groups have reported single wavelength ellipsometry studies of film transformations at electrode surfaces. A summary of such studies is given in a review of applications of ellipsometry in electrochemical systems.[11] From such studies it can be concluded that Δ vs Ψ plots for different ion or charge propagation mechanisms in films have unique shapes. In general, these films have been much thinner than those in our studies. For films that are several hundred nanometers thick, distinction between alternative models is even clearer than for sub-100-nm thick films. To our knowledge, no comparable studies have been done on the partitioning of an absorbing species into a film from solution. Here we summarize simulations of three modes for the partitioning of $Ru(bpy)_3^{2+}$ into Nafion film and show that two are unsuitable for description of our dynamic system. The third, uniform filling of the chromophore in time, is suitable and is used in our analysis of experimental dynamic data.

For digital simulation of a film whose composition varies along its thickness dimension, we divide the film into many smaller thickness layers (sublayers), each of which has constant composition. By varying the compositions of the sublayers in a uniform manner, the collection of them can be made to approximate a graded film's properties. In constructing a global optical model for simulations, a 440-nm thick film was divided into 20 equal sublayers each having a 22-nm thickness. This number of sublayers is sufficient to approximate a film with varying composition.[30]

Three models were simulated, each of which describe different concentration profiles of $Ru(bpy)_3^{2+}$ in the film during partitioning. **Model A** simulates $Ru(bpy)_3^{2+}$ first binding to ion exchange sites close to the film−solution interface and the chromophore diffuses deeper into the film only when all these available sites are taken. For this model a relatively sharp boundary exists that divides the film into regions where chromophore is present, and the rest of the film. This sharp boundary penetrates deeper into the film in time as more and more chromophore partitions into the film.

Concentration profiles that describe a Fickian diffusion process are the bases for **Model B**. This model assumes that the concentration of analyte at the solution−film interface is fixed and chromophores diffuse into the film governed by its diffusion coefficient in the film. The concentration of the chromophore along the film's thickness during the partitioning process was calculated with a finite difference simulation algorithm.[31] For the simulation the film was divided into 96 sublayers. Because only 20 sublayers are used in the global optical model for simulation of ellipsometry results, every fifth layer's (1st, 6^{th},..., 96^{th}) concentration was used for calculation of ellipsometric data.

Model C assumed that concentration of the chromophore increased uniformly throughout the film in time. All three partitioning models are illustrated in Figure 8. In the three

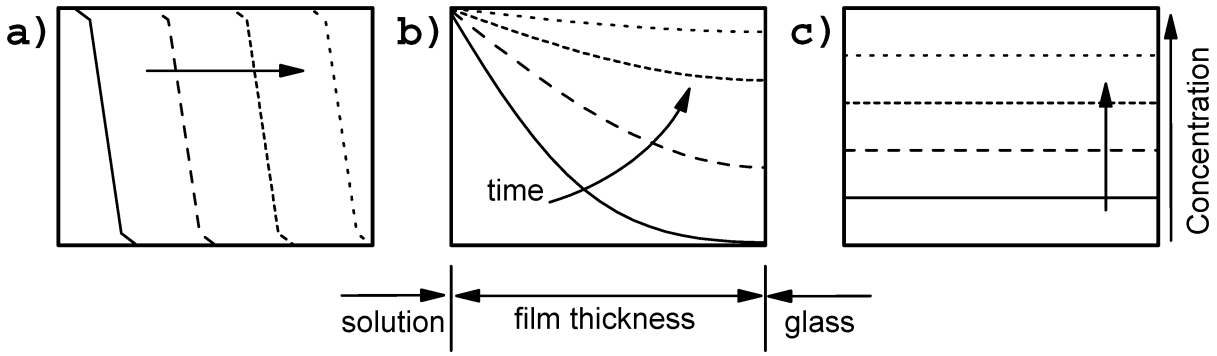

Figure 8. Schematic diagram of the three models of $Ru(bpy)_3^{2+}$ partitioning into the Nafion film: (a) loading of the film by a sharp boundary between unchanged and saturated film that in time moves from the solution−film interface to the film−glass interface; (b) Fickian diffusion model; (c) uniform concentration increase model. Panel labeling corresponds to model labels in text. For each panel, the horizontal axis represents the film thickness dimension and the vertical axis represents $Ru(bpy)_3^{2+}$ concentration as a percent of equilibrium concentration. Left side of the panel coincides with the solution−film interface and the panel's right side is the film−glass interface. Lines in the time sequence (shown by arrows) are as follows: solid (early uptake stage); long dash; short dash; and dotted (near equilibrium).

panels, the horizontal axis represents the film cross-section. On the left side of each panel is the chromophore-bearing solution interface; on the right, the glass interface as illustrated in panel b. The vertical axes in each panel represents concentration of the chromophore in the film expressed as a fraction of the value at equilibrium. The optical constants of a film equilibrated with chromophore solution and a film equilibrated with water were taken as the basis for the calculation of optical constants of the film at intermediate concentrations using the Bruggeman Effective Medium approximation.[21] In this case this approximation simply linearly varies optical constants (e.g., absorbance) with increasing volume fraction of the saturated film. For example, when the concentration of the chromophore in a given sublayer was 30% of its maximum value, the optical constants of this sublayer were calculated as a mix of a water-equilibrated film (70% composition fraction) and a fully loaded film (30% composition fraction).

The trajectories in the Δ vs Ψ plots for the three partitioning models are distinctly different. In Figure 9 such trajectories are plotted for two wavelengths, one at 460 nm near the $Ru(bpy)_3^{2+}$ absorbance maximum (see Figure 3) and one at 700 nm where the chromophore does not absorb. The panels in Figure 9 are labeled according to partitioning models A, B, and C. The starting points and end points for all calculated trajectories (dashed lines) for the same wavelength are the same since the chromophore's concentrations at these points are identical.

Comparing the trajectories for the three models, several conclusions can be reached. First, for the linear uptake Model C, Ψ and Δ change monotonically from their starting values to endpoints. Second, for both Models A and B, characteristic looping is observed. The loops are especially pronounced for Model A, which describes the partitioning process with a sharp moving boundary. Equivalent loops are simply not observed in experimentally acquired data (solid lines). Third, when all simulated trajectories are superimposed (not shown), it is evident that in early stages of the partitioning process Model A and Model B create similar trajectories. Near saturation the behavior of Model B is more similar to Model C than to Model A. This can be rationalized by inspection of the $Ru(bpy)_3^{2+}$ concentration profiles shown in Figure 8; at early times Fickian diffusion Model B has a large concentration gradient inside the film as does Model A, near saturation these gradients become smaller and traces become more similar to linear uptake of Model C where no concentration gradients exist.

Finally, in comparing the simulations with experimental data, it is clear that Model C best describes the concentration of the chromophore $Ru(bpy)_3^{2+}$ in the film. The match between experimental and simulated trajectories in Figure 9, parts 1c and 2c, is not, however, perfect. This was expected since film thickness variation was not included in any of the models. Indeed, the fit of Model C including film thickness variations has been presented in Figure 5. It is interesting to note that the three simulated partitioning models exhibit unique characteristics at both wavelengths, where optical absorption in the film is signif-

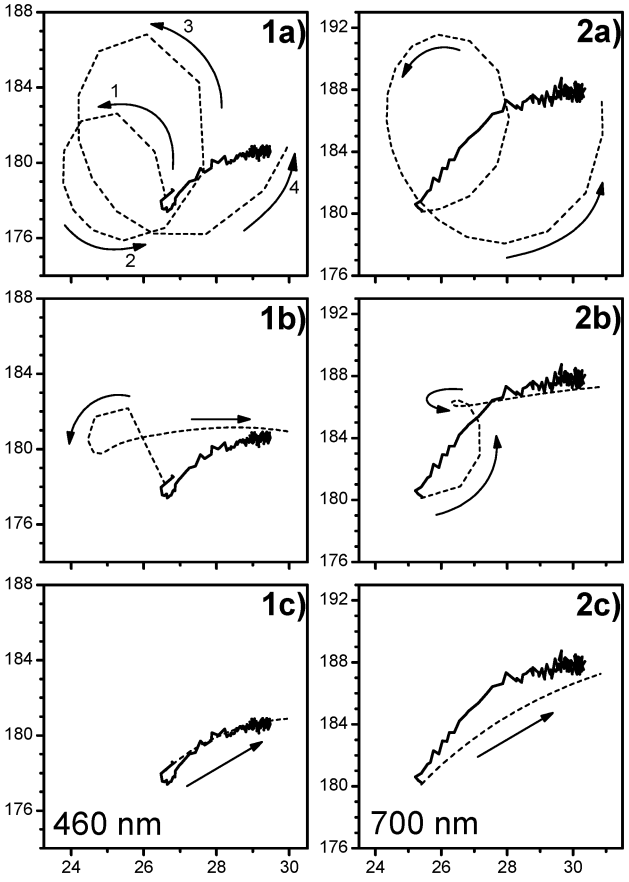

Figure 9. Δ vs Ψ plots for three simulated partitionings at two selected wavelengths. Panels are labeled according to wavelength (1: 460 nm, 2: 700 nm) and partitioning model (A, B, and C, see text or Figure 7 for explanation). For each panel Ψ values are plotted on the horizontal axis and Δ values on the vertical axis. Experimental data are shown with solid lines, calculated with dashed lines. Arrows show direction of change of ellipsometric parameters from the beginning of the experiment towards saturated film.

icant and where the film is completely transparent. This is important because it demonstrates that even the partitioning of nonabsorbing species can be studied as long as there is a significant film refractive index change during the partitioning process.

4. Conclusions

We have presented spectroscopic ellipsometry data describing the dynamics of the partitioning of a model chromophore ($Ru(bpy)_3^{2+}$) into a thin porous solid film (Nafion). Ellipsometric measurements were made through a thick SF11 glass substrate with the Nafion film and chromophore-bearing solution being on the backside of the substrate relative to polarized light interrogation of the system. Spatial separation of the front surface reflection from the back reflection (by the use of a thick glass substrate and an iris) increased measurement sensitivity compared to measurements made with all reflected beams entering the detector. Backside interrogation also permitted the study of the film's optical properties at wavelengths where the bathing solution containing the chromophore significantly absorbed light. Experimental results specifically indicate that the model Nafion film thickness in water increased by 31% compared to its dry state. The thickness increase was accompanied by a refractive index decrease, a change in the direction of water's refractive index.

Data acquired in situ while the model chromophore $Ru(bpy)_3^{2+}$ partitioned into the film were successfully modeled using a globally determined optical multilayer layer model. This global model was constructed by sequential experimental examination of the individual component layers of the system. A quantitative description of the dynamic film was achieved by assembling a model film layer that contained Tauc-Lorentz oscillators to describe both the real and imaginary parts of the refractive index using the Kramer-Kronig relationship. Subsequent analysis of experimental data using the global model resulted in a quantitative description of how the film's optical constants and thickness changed as chromophore $Ru(bpy)_3^{2+}$ partitioned into it from solution. At all investigated wavelengths (from 420 to 1000 nm), the refractive index increased significantly on incorporation of the chromophore. These changes were the largest (up to 0.1 units) at wavelengths near the chromophore absorbance maximum at 453 nm. The corresponding extinction coefficient k reached the high value of 0.055 at the absorbance maximum. The film's thickness also changed, albeit in a more complex manner, during the course of the partitioning. On first incorporation of the chromophore, the film contracted and then, as the film approaches equilibrium with the bathing solution, re-expanded.

Digital simulations of three different chromophore-partitioning modes were presented. Analysis of Δ vs Ψ traces for the three simulated modes strongly supports a simple uniform optical layer model description of the partitioning process for the $Ru(bpy)_3^{2+}$−Nafion film system under the prevailing experimental conditions.

Overall, the results gave new insights into the acquisition of the data for, and associated interpretation of, the chromophore-film partitioning process. Indeed, sensor films such as Nafion are to be thought of as dynamic rather than static systems; their optical and physical properties change significantly with environmental change, including ion exchange. In the longer term, armed with the knowledge gained by these studies and similar studies of film processes, we hope to further understand how to use and to better make useful chemical sensor films.

Acknowledgment. This work was supported by a grant awarded by the Environmental Management Sciences Program of the U.S. Department of Energy, Office of Environmental Management (Grant DE-FG0799ER62331). The purchase of the J.A. Woollam ellipsometer was made possible by a grant from the Hayes Fund of the State of Ohio.

Supporting Information Available: Polishing procedure of glass substrates, overview of optical modeling procedures used to interpret measured ellipsometric parameters, table containing positions and relative magnitudes of oscillators describing $Ru(bpy)_3^{2+}$ absorbance, figures of Ψ and Δ changes vs time during partitioning at selected wavelengths, figure of refractive index and extinction coefficient vs wavelength at various stages of the analyte partitioning, figure of film thickness changes over time for partitioning of $Ru(bpy)_3^{2+}$ into film from aqueous solution (no supporting electrolyte) and comparison of ellipsometric data calculated with model that takes into account absorbance to a model where absorbance is neglected. This material is available free of charge via the Internet at http://pubs.acs.org.

References and Notes

(1) Tatsuma, T.; Ozaki, M.; Oyama, N. *J. Electroanal. Chem.* **1999**, *469*, 34−42.
(2) Shin, M.; Kim, E.-Y.; Kwak, J.; Jeon, I. C. *J. Electroanal. Chem.* **1995**, *394*, 87−92.
(3) Shi, M.; Anson, F. C. *J. Electroanal. Chem.* **1997**, *425*, 117−123.
(4) Tjaernhage, T.; Sharp, M. *Electrochim. Acta* **1994**, *39*, 623−628.
(5) Krtil, P.; Trojanek, A.; Samec, Z. *J. Phys. Chem. B* **2001**, *105*, 7979−7983.
(6) Abraham, S.; Ramaraj, R. *J. Appl. Polym. Sci.* **1997**, *65*, 777−787.
(7) Zhang, Z.; Verma, A. L.; Nakashima, K.; Yoneyama, M.; Iriyama, K.; Ozaki, Y. *Langmuir* **1997**, *13*, 5726−5731.
(8) Kharlampieva, E.; Sukhishvili, S. A. *Langmuir* **2003**, *19*, 1235−1243.
(9) Castellano, F. N.; Heimer, T. A.; Tandhasetti, M. T.; Meyer, G. J. *Chem. Mater.* **1994**, *6*, 1041−1048.
(10) Collinson, M. M.; Novak, B. *J. Sol.-Gel Sci. Technol.* **2002**, *23*, 215−220.
(11) Gottesfeld, S.; Kim, Y.-T.; Redondo, A. Recent Applications of Ellipsometry and Spectroellipsometry in Electrochemical Systems. In *Physical Electrochemistry*; Rubinstein, I., Ed.; Marcel Dekker: New York, 1995; 393−467.
(12) Shi, Y.; Slaterbeck, A. F.; Seliskar, C. J.; Heineman, W. R. *Anal. Chem.* **1997**, *69*, 3679−3686.
(13) Shi, Y.; Seliskar, C. J.; Heineman, W. R. *Anal. Chem.* **1997**, *69*, 4819−4827.
(14) Shi, Y.; Seliskar, C. J. *Chem. Mater.* **1997**, *9*, 821−829.
(15) Gao, L.; Seliskar, C. J. *Chem. Mater.* **1998**, *10*, 2481−2489.
(16) Zudans, I.; Seliskar, C. J.; Heineman, W. R. *Thin Solid Films* **2003**, *426*, 238−245.
(17) Johs, B.; Woollam, J. A.; Herzinger, C. M.; Hilfiker, J.; Synowicki, R.; Bungay, C. L. *Crit. Rev. Opt. Sci. Technol.* **1999**, *CR72*, 29−58.
(18) Woollam, J. A.; Johs, B.; Herzinger, C. M.; Hilfiker, J.; Synowicki, R.; Bungay, C. L. *Crit. Rev. Opt. Sci. Technol.* **1999**, *CR72*, 3−28.
(19) Zudans, I. In Situ Studies of Sensor Film Dynamics by Spectroscopic Ellipsometry. Ph.D. Thesis, University of Cincinnati, OH, August 2003.
(20) Azzam, R. M. A.; Bashara, N. M. *Ellipsometry and Polarized Light*; Elsevier Science: Amsterdam, The Netherlands, 1977.
(21) Tompkins, H. G.; McGahan, W. A. *Spectroscopic Ellipsometry and Reflectometry: a User's Guide*; John Wiley: New York, 1998.
(22) Hayfield, P. C. S.; White, G. W. T. An Assessment of the Suitability of the Drude-Tronstad Polarised Light Method for the Study of Film Growth on Polycrystalline Metals. In *Ellipsometry in the Measurement of Surfaces and Thin Films*; Passaglia, E., Stromberg, R. R., Kruger, J., Eds.; National Bureau of Standards Miscellaneous Publication 256; U.S. Government Printing Office: Washington, DC, 1964; pp 157−199.
(23) *Handbook of Optical Constants of Solids II*; Palik, E. D., Ed.; Academic Press: Boston, 1991.
(24) Walsby, N.; Hietala, S.; Maunu, S. L.; Sundholm, F.; Kallio, T.; Sundholm, G. *J. Appl. Polym. Sci.* **2002**, *86*, 33−42.
(25) Nandan, D.; Mohan, H.; Iyer, R. M. *J. Membr. Sci.* **1992**, *71*, 69−80.
(26) Morris, D. R.; Sun, X. *J. Appl. Polym. Sci.* **1993**, *50*, 1445−1452.
(27) Yeo, R. S.; Cheng, C. H. *J. Appl. Polym. Sci.* **1986**, *32*, 5733−5741.
(28) Gebel, G.; Aldebert, P.; Pineri, M. *Polymer* **1993**, *34*, 333−339.
(29) Jellison, G. E., Jr.; Modine, F. A. *Appl. Phys. Lett.* **1996**, *69*, 371−373.
(30) Piel, J. P. *Thin Solid Films* **1993**, *234*, 451−453.
(31) Britz, D. *Digital Simulation in Electrochemistry*, 2nd ed.; Springer-Verlag: New York, 1988.